LETTER

doi:10.1038/nature13287

Human oocytes reprogram adult somatic nuclei of a type 1 diabetic to diploid pluripotent stem cells

Mitsutoshi Yamada[1]*, Bjarki Johannesson[1]*, Ido Sagi[2], Lisa Cole Burnett[3], Daniel H. Kort[4,5], Robert W. Prosser[4,5], Daniel Paull[1], Michael W. Nestor[1], Matthew Freeby[3], Ellen Greenberg[3], Robin S. Goland[3], Rudolph L. Leibel[3], Susan L. Solomon[1], Nissim Benvenisty[2], Mark V. Sauer[4,5] & Dieter Egli[1]

The transfer of somatic cell nuclei into oocytes can give rise to pluripotent stem cells that are consistently equivalent to embryonic stem cells[1–3], holding promise for autologous cell replacement therapy[4,5]. Although methods to induce pluripotent stem cells from somatic cells by transcription factors[6] are widely used in basic research, numerous differences between induced pluripotent stem cells and embryonic stem cells have been reported[7–11], potentially affecting their clinical use. Because of the therapeutic potential of diploid embryonic stem-cell lines derived from adult cells of diseased human subjects, we have systematically investigated the parameters affecting efficiency of blastocyst development and stem-cell derivation. Here we show that improvements to the oocyte activation protocol, including the use of both kinase and translation inhibitors, and cell culture in the presence of histone deacetylase inhibitors, promote development to the blastocyst stage. Developmental efficiency varied between oocyte donors, and was inversely related to the number of days of hormonal stimulation required for oocyte maturation, whereas the daily dose of gonadotropin or the total number of metaphase II oocytes retrieved did not affect developmental outcome. Because the use of concentrated Sendai virus for cell fusion induced an increase in intracellular calcium concentration, causing premature oocyte activation, we used diluted Sendai virus in calcium-free medium. Using this modified nuclear transfer protocol, we derived diploid pluripotent stem-cell lines from somatic cells of a newborn and, for the first time, an adult, a female with type 1 diabetes.

We have previously reported the derivation of pluripotent stem cells containing a reprogrammed genome derived from an adult somatic cell, and a haploid oocyte genome[12]. Development to the blastocyst stage only occurred in the presence of the oocyte genome; diploid nuclear transfer cells arrested development at the cleavage stages, failing to express embryonic genes. To improve developmental potential and transcriptional reprogramming in diploid nuclear transfer oocytes, we tested the effect of histone deacetylation (HDAC) inhibitors, as well as changes to the artificial activation protocol on developmental potential. These modifications were based on the report that HDAC inhibitors improved development after somatic cell nuclear transfer in mouse oocytes[13], and on our observation that parthenogenetic development was more efficient when oocytes were activated with the translation inhibitor puromycin[14] than when activated with the kinase inhibitor 6-dimethylaminopurine (6-DMAP)[12] (Extended Data Fig. 1). To minimize the effect of potential variation in oocyte quality, for each condition we used oocytes from at least four donors (Fig. 1a). We first tested the use of puromycin for oocyte activation in somatic cell nuclear transfer without removing the oocyte genome, resulting in efficient development to the blastocyst stage (Fig. 1a). However, development of diploid nuclear transfer oocytes still arrested at cleavage stages (Fig. 1a). Only when we applied the HDAC inhibitor scriptaid during the first embryonic interphase, did we observe development to the morula and blastocyst stages at a low frequency (Fig. 1a). Further improvement in developmental potential was observed when both puromycin and 6-DMAP were combined during oocyte activation, resulting in development to expanded blastocysts (Fig. 1a, b and Extended Data Fig. 2a, b). Puromycin promotes oocyte activation by inhibiting translation of cyclin B[15,16], whereas 6-DMAP inhibits the activity of meiotic kinases; their combined use may result in a more complete or more rapid inactivation of meiotic kinases. These results show that an improved activation protocol and the use of an HDAC inhibitor enabled development of nuclear transfer cells to the blastocyst stage in the absence of the oocyte genome.

Because development beyond the cleavage stage requires gene expression[17], development to the morula and blastocyst stages indicates transcriptional activity of the transferred somatic cell genome. Whereas previous nuclear transfer protocols did not result in expression of a green fluorescent protein (GFP) transgene contained in the somatic cell genome[12], 58% (14 of 24) of the nuclear transfer cells treated with HDAC inhibitor were GFP positive (Fig. 1b), and had a global gene expression profile similar to *in vitro* fertilized (IVF) embryos (Fig. 1c), demonstrating that transcriptional reprogramming was extensive. Of the 7 nuclear transfer blastocysts obtained using optimized protocols, 3 formed an outgrowth (Extended Data Fig. 2c), but none gave rise to an embryonic stem (ES) cell line.

More recently, it has become possible to derive diploid pluripotent stem-cell lines from fetal fibroblasts[18]. The derivation of cell lines from an 8-month-old subject with Leigh syndrome was also stated, although no karyotype or evidence of pluripotency was provided. While the use of the HDAC inhibitor to obtain blastocyst development is consistent with our data and a previous report[19], the authors also attributed successful derivation to the use of caffeine during oocyte enucleation to promote nuclear envelope breakdown and condensation of somatic chromatin, the use of a hormone stimulation protocol yielding a small number of high-quality oocytes, and to the use of an electrical pulse for oocyte activation. As it remained unclear whether diploid nuclear transfer ES cells could reliably be derived from postnatal somatic cells, we determined the requirements for blastocyst development and ES cell derivation using adult somatic cells of a type 1 diabetic female (age 32 years, age of onset 10 years) and human foreskin fibroblasts of a male newborn for nuclear transfer.

We first determined whether oocyte enucleation interfered with the condensation of transferred somatic chromatin, a process correlating with developmental potential[20]. When we transferred somatic cell genomes at G1 or G0 stages of the cell cycle into enucleated oocytes, 17 out of 23 (74%) assembled a spindle within 1–4 h after transfer as determined by microtubule birefringence[21] or immunostaining (Fig. 2a). Somatic chromosomes were condensed and phosphorylated on serine 28 of histone H3, but not aligned on a metaphase plate, because unreplicated

[1]The New York Stem Cell Foundation Research Institute, New York, New York 10032, USA. [2]Stem Cell Unit, Department of Genetics, Silberman Institute of Life Sciences, The Hebrew University of Jerusalem, Jerusalem 91904, Israel. [3]Naomi Berrie Diabetes Center, Department of Pediatrics, College of Physicians and Surgeons, Columbia University, New York, New York 10032, USA. [4]Center for Women's Reproductive Care, College of Physicians and Surgeons, Columbia University, New York 10019, USA. [5]Department of Obstetrics and Gynecology, College of Physicians and Surgeons, Columbia University, New York 10032, USA.

*These authors contributed equally to this work.

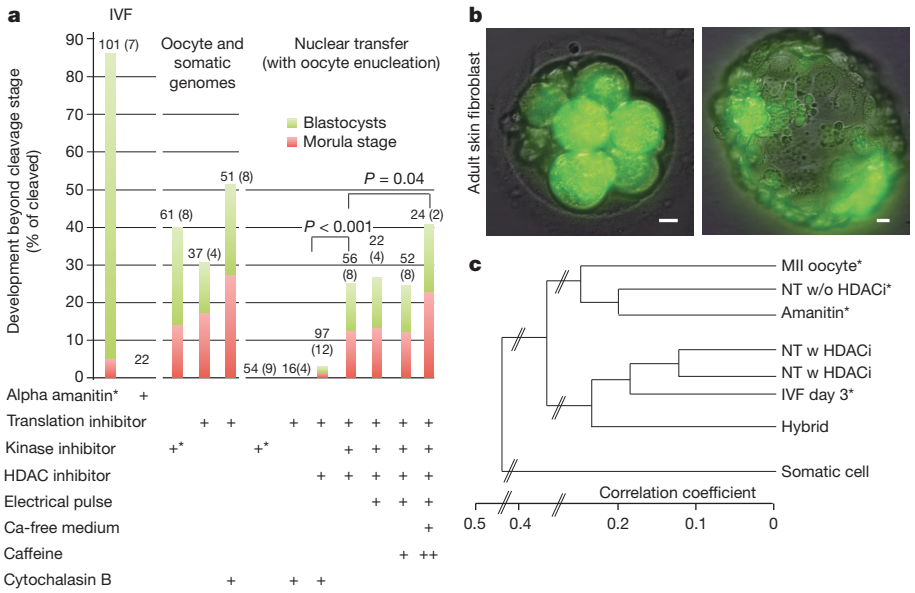

Figure 1 | Developmental potential of somatic cell nuclear transfer oocytes. **a**, Percentage of oocytes developing beyond the cleavage stage. The total number of oocytes and the number of oocyte donors (in parenthesis) contributing to a particular experiment is indicated above each column. ++, Caffeine was also added during oocyte transport. Statistical analysis was done using Chi-square test. **b**, Expression of a GFP transgene from the transferred somatic cell genome, at the cleavage stage and at the blastocyst stage. **c**, Cluster analysis of global gene expression profile after nuclear transfer of adult somatic cells, as well as oocytes and IVF embryos. *Data with an asterisk are from refs 12 and 27 for comparison. Scale bars, 10 μm. HDACi, HDAC inhibitor; NT, nuclear transfer.

chromosomes cannot form bipolar amphitelic attachments, as in a spindle of the MII oocyte (Fig. 2b). Although chromosome condensation did not occur in all oocytes receiving a somatic cell genome, this was not due to the enucleation procedure. Chromosome condensation and spindle assembly occurred with similar efficiency after transfer of a somatic cell genome into non-enucleated oocytes (10/13, 77%). Two non-enucleated oocytes that failed to assemble a spindle around somatic chromatin showed no phosphorylation of somatic histones (Fig. 2c), and segregation of the oocyte genome with the formation of a midbody positive for borealin (Fig. 2d), a component of the chromosome passenger complex localizing to the midbody at anaphase[22].

Because a rise in intracellular calcium concentration is a potent inducer of anaphase in oocytes, we investigated the effect of Sendai virus used for somatic cell fusion on intracellular calcium levels. Intact oocytes and karyoplasts—the by-product of oocyte enucleation—were equilibrated with the calcium indicator dye Fluo-4 and exposed to Sendai virus. Within minutes, an increase of Fluo-4 fluorescence was observed (Fig. 2e–h and Extended Data Fig. 3). Fluorescence was calcium-dependent, as oocytes incubated in calcium-free media showed decreased fluorescence compared to oocytes incubated in calcium-rich media (Extended Data Fig. 3). These results show that the fusion of somatic cells using Sendai virus can increase calcium influx and compromise the integrity of meiotic arrest. Therefore, nuclear transfer experiments from all but four oocyte donations were performed using Sendai virus diluted up to 20-fold. And in two donations, calcium was omitted from the medium used for nuclear transfer, as well as during incubation before oocyte activation. The absence of calcium in the medium was compatible with condensation of transferred somatic chromatin, resulting in efficient development to the blastocyst stage (Fig. 1a and Extended Data Fig. 4). Technical changes adapted from ref. 18, including an electrical pulse

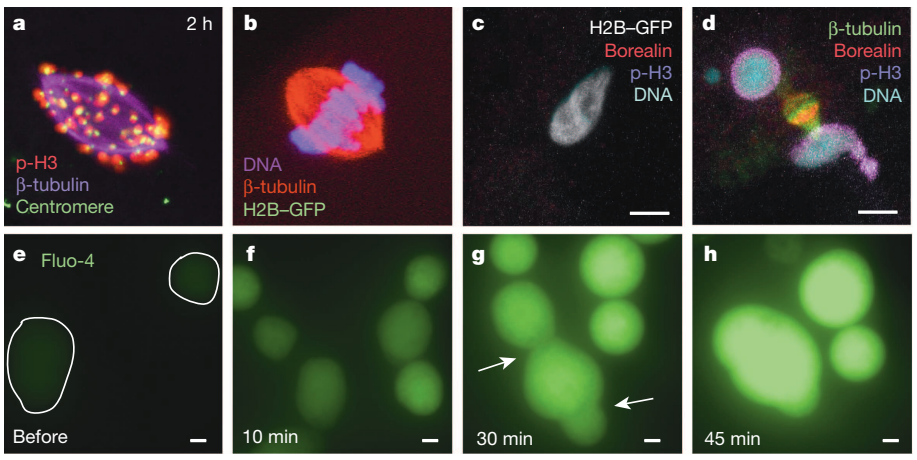

Figure 2 | Chromosome condensation and spindle assembly after somatic cell nuclear transfer. **a**, Spindle assembly on a somatic G1/G0 genome. Time indicates hours post transfer. p-H3, phosphorylated histone H3. **b**, Spindle of the human MII oocyte. **c**, Somatic nucleus transferred into the oocyte using undiluted Sendai virus. Note the lack of phosphorylated histone H3. **d**, Oocyte genome in the same egg. Note the segregation of oocyte chromosomes. **e–h**, Fluorescence time course of the calcium indicator dye Fluo-4 in oocyte karyoplasts before and after incubation with fusogenic Sendai virus (less than 20 s). Time after exposure is indicated. Arrows point to sites of fusion. Scale bar, 5 μm.

for oocyte activation and the use of caffeine during oocyte manipulation were most effective when combined with omitting calcium from the manipulation medium (Fig. 1a).

For the derivation of nuclear transfer ES (NT-ES) cell lines, we added fetal bovine serum (FBS) to the embryo culture and derivation media[18]. FBS promoted the formation of an inner cell mass at the expense of trophectoderm cells. Of eight nuclear transfer blastocysts generated without the addition of FBS, two contained exclusively (60 or more) trophectoderm cells (Extended Data Fig. 5a), and none gave rise to an ES cell line. In the presence of FBS, even blastocysts with a small number of cells formed a distinct inner cell mass (four out of four), with fewer than 20 trophectoderm cells (Extended Data Fig. 5a). Three out of four such blastocysts formed an outgrowth (Extended Data Fig. 5b) and developed into three cell lines containing a diploid male karyotype derived from foreskin fibroblasts (Extended Data Fig. 6). A NT-ES cell line with a diploid female karyotype was also derived from an adult somatic cell of a type 1 diabetic (Fig. 3a). All four cell lines expressed markers of pluripotency (Fig. 3b–d and Extended Data Fig. 6a–c), and lacked markers of the dermal fibroblasts (Fig. 3e). In an analysis of global gene expression patterns, NT-ES cells clustered closely with other human pluripotent stem cells, including ES cells from fertilized embryos and induced pluripotent stem (iPS) cells (Fig. 3f). In embryoid bodies and upon transplantation into immunocompromised mice, all four NT-ES cell lines gave rise to cell types of three germ layers (Fig. 3g and Extended Data Fig. 7). When exposing them to a combination of cellular patterning factors (see Methods), we found efficient differentiation into neurons (Fig. 3h), pancreatic and duodenal homeobox-1 (PDX1)-positive cells (Fig. 3i), and insulin-positive cells (Fig. 3j) that were able to secrete insulin into the medium upon potassium stimulation (Fig. 3k).

Although nuclear transfer blastocysts could be obtained with an efficiency of approximately 10%, developmental efficiency varied between different oocyte donors, even when other aspects of the nuclear transfer protocol were kept constant. To better understand the source of the variation in oocyte performance, we retrospectively assessed the effect of patient age and hormone stimulation protocol on developmental potential after nuclear transfer (Extended Data Fig. 8, 154 oocytes obtained from 18 donors contained in the last four columns of Fig. 1a). In contrast to a previous report[18], we found no association between the number of MII oocytes retrieved per donation and developmental competence (Extended Data Fig. 8b). In fact, the derivation of a NT-ES cell line from adult somatic cells was achieved using 9 oocytes selected randomly from a total of 31 MII oocytes obtained in a single donation. Oocytes from subjects age 21–26 years showed greater developmental potential compared to subjects age 27–32 years, consistent with data

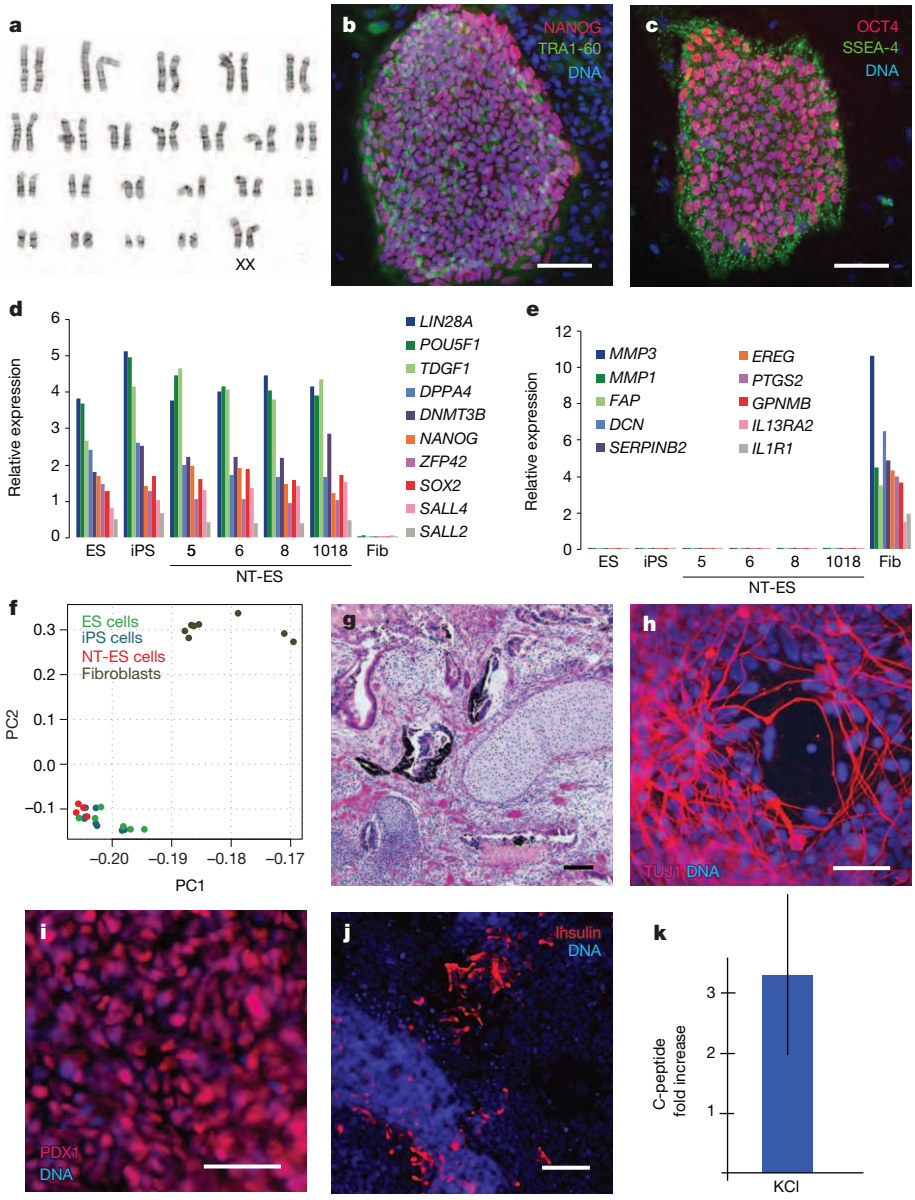

Figure 3 | Derivation of diploid NT-ES cells from adult somatic cells. **a–c**, **g–k**, Characterization of a NT-ES cell line derived from adult somatic cells of a female type 1 diabetic (ID 1018). **a**, Karyotype. **b**, **c**, Expression of pluripotency markers. **d**, **e**, Microarray analysis of NT-ES cell lines NT-ES5, NT-ES6, NT-ES8 (neonatal) and NT-ES 1018 (adult), and of fibroblasts (Fib), ES and iPS cells. **d**, Expression of pluripotency markers. **e**, Expression of fibroblast-specific genes. **f**, Principal component (PC) analysis of global gene expression patterns of NT-ES cells, ES cells from normally fertilized embryos, iPS cells and fibroblasts. Sample identity is provided in Extended Data Table 1. **g**, Teratoma analysis. **h**, Directed differentiation into neurons. **i**, **j**, Directed differentiation of NT-ES cells from a type 1 diabetic into pancreatic precursor cells (**i**) and insulin-producing cells (**j**). **k**, Insulin secretion upon stimulation with potassium. Bar indicates standard error of $n = 4$. Scale bar, 50 µm.

from clinical donor IVF cycles[23]. We observed no significant effect of the method of pituitary downregulation as gonadotropin releasing hormone (GnRH) antagonist and GnRH agonist protocols resulted in development to the blastocyst stage. We also observed no significant effect of the daily dose of gonadotropin used for stimulation. However, there was a trend towards a negative effect of the total duration (days) of gonadotropin stimulation required to reach a follicular size of 18 mm (Extended Data Fig. 8b). Although prolonged stimulation has been suspected to be a negative predictor of IVF outcome, clinical pregnancy rates have not been shown to be affected[24]. Thus, additional requirements for somatic cell reprogramming may reveal subtle biological differences that are not readily apparent in clinical IVF.

This retrospective analysis also revealed that one of the most relevant technical parameters for efficient blastocyst development was the use of diluted Sendai virus for fusion, whereas the use of FBS was most relevant for ES cell derivation (Extended Data Fig. 8c, d). Surprisingly, development to the blastocyst stage was equally efficient when either neonatal or adult fibroblasts were used for transfer.

Our results show that technical improvements enable development to the blastocyst stage after transfer of adult somatic cells. These changes obviated the requirement for the oocyte genome, although development with the oocyte genome remained more efficient (Fig. 1a). One interpretation of the beneficial effect of the oocyte genome is that it compensates for incomplete reprogramming of somatic chromatin. Future studies should lead to a better understanding of the molecular mechanisms of how these technical improvements affect reprogramming and developmental outcome.

In summary, we have demonstrated the derivation of human ES cells from neonatal and adult somatic cells by nuclear transfer. The stem cells are pluripotent and could be differentiated into insulin-producing beta cells, the cell type lost in patients with type 1 diabetes. These stem cells could therefore be used to generate cells for therapeutic cell replacement. Although it is now possible to induce stem-cell formation by overexpression of embryonic transcription factors[6], these cells are often differentiation-defective[7], contain aberrant patterns of cytosine methylation[9,10,25] and hydroxymethylation[8], acquire somatic coding mutations[26], and show biallelic expression of imprinted genes[11]. Studies comparing nuclear transfer ES cells to iPS cells of isogenic origin should enable evaluation of the quality of cells generated by different methods of reprogramming.

METHODS SUMMARY

Nuclear transfer was performed using somatic cells grown to confluence and cultured in 0.5% serum for 2–5 days before transfer to induce cell cycle arrest in G1/G0. Oocytes were enucleated either before or after transfer using microtubule birefringence[21] and somatic cells were fused to the oocyte using diluted Sendai virus, in calcium-free medium. Upon completion of the manipulation, oocytes were incubated for 45 min–1 h in calcium-free MCZB, then placed in calcium-containing medium for 10 min before activation. Oocyte activation was performed using electrical pulses, followed by 4 h incubation in medium containing 10 $\mu g\,ml^{-1}$ puromycin and 2 mM 6-DMAP as well as HDAC inhibitors scriptaid and nch51. HDAC inhibitor was retained for a total of 15 h during the first cell cycle. Culture to the blastocyst stage and ES cell derivation was performed containing 10%FBS tested for compatibility with growth of human ES cells. A detailed protocol for embryonic stem-cell derivation by somatic cell nuclear transfer into human oocytes is available on the *Nature* Protocol Exchange website (http://dx.doi.org/10.1038/protex.2014.013)[28].

Online Content Any additional Methods, Extended Data display items and Source Data are available in the online version of the paper; references unique to these sections appear only in the online paper.

Received 4 February; accepted 27 March 2014.
Published online 28 April 2014.

1. Kim, K. *et al.* Epigenetic memory in induced pluripotent stem cells. *Nature* **467,** 285–290 (2010).
2. Brambrink, T., Hochedlinger, K., Bell, G. & Jaenisch, R. ES cells derived from cloned and fertilized blastocysts are transcriptionally and functionally indistinguishable. *Proc. Natl Acad. Sci. USA* **103,** 933–938 (2006).
3. Wakayama, S. *et al.* Equivalency of nuclear transfer-derived embryonic stem cells to those derived from fertilized mouse blastocysts. *Stem Cells* **24,** 2023–2033 (2006).
4. Tabar, V. *et al.* Therapeutic cloning in individual parkinsonian mice. *Nature Med.* **14,** 379–381 (2008).
5. Rideout, W. M. III, Hochedlinger, K., Kyba, M., Daley, G. Q. & Jaenisch, R. Correction of a genetic defect by nuclear transplantation and combined cell and gene therapy. *Cell* **109,** 17–27 (2002).
6. Takahashi, K. *et al.* Induction of pluripotent stem cells from adult human fibroblasts by defined factors. *Cell* **131,** 861–872 (2007).
7. Koyanagi-Aoi, M. *et al.* Differentiation-defective phenotypes revealed by large-scale analyses of human pluripotent stem cells. *Proc. Natl Acad. Sci. USA* **110,** 20569–20574 (2013).
8. Wang, T. *et al.* Subtelomeric hotspots of aberrant 5-hydroxymethylcytosine-mediated epigenetic modifications during reprogramming to pluripotency. *Nature Cell Biol.* **15,** 700–711 (2013).
9. Ohi, Y. *et al.* Incomplete DNA methylation underlies a transcriptional memory of somatic cells in human iPS cells. *Nature Cell Biol.* **13,** 541–549 (2011).
10. Ruiz, S. *et al.* Identification of a specific reprogramming-associated epigenetic signature in human induced pluripotent stem cells. *Proc. Natl Acad. Sci. USA* **109,** 16196–16201 (2012).
11. Pick, M. *et al.* Clone- and gene-specific aberrations of parental imprinting in human induced pluripotent stem cells. *Stem Cells* **27,** 2686–2690 (2009).
12. Noggle, S. *et al.* Human oocytes reprogram somatic cells to a pluripotent state. *Nature* **478,** 70–75 (2011).
13. Van Thuan, N. *et al.* The histone deacetylase inhibitor scriptaid enhances nascent mRNA production and rescues full-term development in cloned inbred mice. *Reproduction* **138,** 309–317 (2009).
14. Paull, D. *et al.* Nuclear genome transfer in human oocytes eliminates mitochondrial DNA variants. *Nature* **493,** 632–637 (2013).
15. Winston, N. J. Stability of cyclin B protein during meiotic maturation and the first mitotic cell division in mouse oocytes. *Biol. Cell* **89,** 211–219 (1997).
16. Stern, S., Rayyis, A. & Kennedy, J. F. Incorporation of amino acids during maturation *in vitro* by the mouse oocyte: effect of puromycin on protein synthesis. *Biol. Reprod.* **7,** 341–346 (1972).
17. Braude, P., Bolton, V. & Moore, S. Human gene expression first occurs between the four- and eight-cell stages of preimplantation development. *Nature* **332,** 459–461 (1988).
18. Tachibana, M. *et al.* Human embryonic stem cells derived by somatic cell nuclear transfer. *Cell* **153,** 1228–1238 (2013).
19. Fan, Y. *et al.* Derivation of cloned human blastocysts by histone deacetylase inhibitor treatment after somatic cell nuclear transfer with beta-thalassemia fibroblasts. *Stem Cells Dev.* **20,** 1951–1959 (2011).
20. Wakayama, T., Perry, A. C., Zuccotti, M., Johnson, K. R. & Yanagimachi, R. Full-term development of mice from enucleated oocytes injected with cumulus cell nuclei. *Nature* **394,** 369–374 (1998).
21. Liu, L., Oldenbourg, R., Trimarchi, J. R. & Keefe, D. L. A reliable, noninvasive technique for spindle imaging and enucleation of mammalian oocytes. *Nature Biotechnol.* **18,** 223–225 (2000).
22. Gassmann, R. *et al.* Borealin: a novel chromosomal passenger required for stability of the bipolar mitotic spindle. *J. Cell Biol.* **166,** 179–191 (2004).
23. Cohen, M. A., Lindheim, S. R. & Sauer, M. V. Donor age is paramount to success in oocyte donation. *Hum. Reprod.* **14,** 2755–2758 (1999).
24. Bar-Hava, I. *et al.* Controlled ovarian hyperstimulation: does prolonged stimulation justify cancellation of *in vitro* fertilization cycles? *Gynecol. Endocrinol.* **21,** 232–234 (2005).
25. Lister, R. *et al.* Hotspots of aberrant epigenomic reprogramming in human induced pluripotent stem cells. *Nature* **471,** 68–73 (2011).
26. Gore, A. *et al.* Somatic coding mutations in human induced pluripotent stem cells. *Nature* **471,** 63–67 (2011).
27. Egli, D. *et al.* Reprogramming within hours following nuclear transfer into mouse but not human zygotes. *Nature Commun.* **2,** 488 (2011).
28. Egli, D. & Chia, G. A protocol for embryonic stem cell derivation by somatic cell nuclear transfer into human oocytes. *Protocol Exch.* http://dx.doi.org/10.1038/protex.2014.013 (2014).

Acknowledgements This research was supported the New York Stem Cell Foundation (NYSCF) and a New York State Stem Cell Science (NYSTEM) IIRP Award no. C026184, and the Russell Berrie Foundation Program in Cellular Therapies of Diabetes. We thank S. Mitalipov for helpful discussions and providing reagents, S. Micucci for counting cells in S-phase, and Z. Hall for critical reading of the manuscript. D.E. is a NYSCF-Robertson Investigator.

Author Contributions M.V.S. supervised the research oocyte donation program and retrieved oocytes. D.E. designed, performed and interpreted nuclear transfer experiments, derived ES cells with M.Y., and wrote the paper with input from all authors. M.Y. performed statistical analysis, M.Y. and B.J. performed stem cell characterization and differentiation, L.C.B. performed neuronal differentiation, I.S. and N.B. performed gene expression analysis, M.W.N. assisted with calcium experiments, D.H.K. performed data analysis, D.P. assisted in nuclear transfer experiments, R.W.P. collected developmental data of IVF embryos, M.F. made the skin biopsy, E.G. coordinated human subjects research, R.S.G. wrote the IRB protocol, R.L.L. contributed project planning, S.L.S. created the environment specifically for this work.

Author Information Microarray data are available at GEO under accession numbers GSE54849 and GSE54876. Reprints and permissions information is available at www.nature.com/reprints. The authors declare no competing financial interests. Readers are welcome to comment on the online version of the paper. Correspondence and requests for materials should be addressed to D.E. (d.egli@nyscf.org).

METHODS

A detailed protocol for embryonic stem-cell derivation by somatic cell nuclear transfer into human oocytes is available on the *Nature* Protocol Exchange website (http://dx.doi.org/10.1038/protex.2014.013)[28].

Research subjects. Oocytes were obtained as previously reported[12,14]. In brief, oocyte donors were recruited from the oocyte donation program at the Center for Women's Reproductive Care (CWRC) at Columbia University College of Physicians and Surgeons. Potential participants discussed the research with a physician and were offered study participation. Upon choosing to donate for research, subjects gave signed informed consent for the study protocol and the use of their oocytes in nuclear transfer research. During a period of three years and four months, 35 subjects donated a total of 512 mature MII oocytes, (average = 14.63 oocytes per cycle, range = 2–31 oocytes per cycle). 423 of these oocytes were used for developmental analyses after somatic cell nuclear transfer reported here. Six of the donors had one or more previous pregnancies, and five had previously donated for reproductive purposes. There were no repeat donations for this study.

Both GnRH antagonist ($n = 33$) and GnRH agonist ($n = 2$) protocols were used. The GnRH antagonist protocol was performed by administering daily subcutaneous rFSH (recombinant follicle stimulating hormone) injections starting on day 2 of the menstrual cycle and the addition of daily GnRH antagonist (Ganirelix) starting on day 6 of stimulation. Final oocyte maturation was triggered after reaching a follicle size of 18 mm with 4 mg GnRH agonist (Lupron) and 1,000 IU hCG (human chorionic gonadotropin, Novarel).

The GnRH agonist protocol was performed by administering daily GnRH agonist for at least 14 days followed by daily rFHS injections. Final maturation trigger was performed by administering 10,000 IU hCG.

For both agonist and antagonist protocols, the dose of rFSH generally consisted of 2 ampoules a day (range 1–3, average 2.49) and the time of stimulation was 10 days (range 9–13 days, average 10.29). Initial dose was established clinically based on subject age, baseline antral follicle count, and anti-mullerian hormone (AMH) level. Dose adjustments and the total days of stimulation were adjusted individually based on follicle number and size and serum oestradiol (E2) levels. Hormones were administered by clinical staff, to ensure consistent application.

At the time of oocyte retrieval, venipuncture was performed for DNA isolation. All oocyte donors obtained compensation for time and effort of $8,000 (before taxation). Such payment is made based on the knowledge that oocyte donors are unlikely to donate oocytes without a form of compensation[29–31], and based on the ethical guidelines of the ASRM and ISSCR[32,33]. Skin biopsies were made using the AccuPunch Biopsy kit (Acuderm Inc.) and somatic cells grown out as previously described[12]. Skin biopsy donors gave signed informed consent. All human subjects research was reviewed by the institutional review board and stem-cell committees of Columbia University.

Oocyte manipulations. Oocytes were retrieved 35 h post induction of ovulation, between 7:30 and 8am. Oocytes were denuded and transported to the laboratory in GMOPSplus (Vitrolife) in a portable incubator heated to 37 °C, arriving no later than 9am. From the scheduled beginning of oocyte retrieval to the time of arrival in the laboratory and starting manipulations, 75 90 min passed. Oocytes were placed on a stage heated to 37 °C, in medium containing 5 μg ml^{-1} cytochalasin B, and enucleated using microtubule birefringence (Oosight) as described[12,21]. Nuclear transfer was performed by fusion of somatic cells to oocytes using inactivated Sendai virus (GenomeOne, Cosmo Bio) resuspended in 260 μl suspension buffer, as described[34], and then further diluted 1:10 to 1:20 in suspension medium, or 1:5 in fusion medium. Foreskin human fibroblasts (BJ) of a newborn were obtained from Stemgent (G00003, cell line 2, passage 6). Somatic cells of type 1 diabetic subject (ID 1018, age at study 32 years, age of onset 10 years) were transduced with a Lentivirus expressing GFP constitutively under the CAGGS promoter. Somatic cells were grown to confluence and cultured in 0.5% serum for 2–5 days before transfer. Analysis of the somatic donor cell population using 5-ethynyl-2′-deoxyuridine (EdU) staining revealed that 0.4% (9 out of 2,121 cells) were in S-phase. The somatic cell was placed in Sendai virus for 10–20 s, then inserted below the zona pellucida, and fusion was confirmed within 5–10 min. Dilution of Sendai virus at 10× had a 100% fusion efficiency, whereas 20× dilution required occasional re-transfer, and a dilution of 40× was unreliable for fusion. 1–3 h post fusion, oocytes were activated using 3 μM ionomycin in Global total (IVF online LGTF-050) for 5 min at 37 °C, followed by culture in 10 μM puromycin, 2 mM 6-DMAP, as well as the histone deacetylase (HDAC) inhibitors scriptaid (250 nM, Sigma S7817) and nch51 (1 μM, Tocris Bioscience 3747), or trichostatin A at 10 nM instead of these two, for 4 to 4.5 h. Cytochalasin B was added in combination with puromycin (Fig. 1a) during the first four hours of artificial activation to inhibit polar body extrusion. Activated constructs were cultured in HDAC inhibitor for an additional 10–16 h, followed by culture in Global total medium. Culture was performed in a MINC incubator fed with gas containing 6% CO2, 5% oxygen and 89% nitrogen. Additional modifications were introduced as described in ref. 18. Caffeine at 1 mM concentration was used during enucleation and somatic cell fusion. Oocytes were activated within approximately an hour post transfer using 4 pulses of 50 μs width at 2.7 kV cm^{-1} in D-sorbitol (0.25 M) containing fusion medium using an LF201 pulser (Nepagene). Activated oocytes were cultured in Global total containing 10% FBS (quality controlled for compatibility with human ES cell growth and rhesus monkey nuclear transfer development by S.Mitalipov[18]) and HDAC inhibitor for 12 h, followed by culture to the blastocysts stage in medium containing 10% FBS.

The derivation of nuclear transfer ES cell lines from BJ fibroblasts at passage 11 was performed using nuclear transfer 30 min before the removal of the oocyte genome in the presence of 1 mM caffeine. Derivation of the adult cell NT-ES cell line was performed using somatic cells at passage 8, from a female subject with T1D (ID-1018, age of onset 10 years, age at study 32 years). Oocytes were transported in GMOPSplus (a medium containing calcium) containing 1 mM caffeine . Upon completion of the manipulation in calcium-free HCZB, oocytes were incubated for 45 min–1 h in calcium-free MCZB, then placed in calcium-containing medium for 10 min before activation and culture as described above. For media formulations of MCZB and HCZB see[35]. Oocyte activation was performed within 2 h post transfer using 4 electrical pulses, followed by incubation in medium containing HDAC inhibitors scriptaid and nch51, in addition to 10 μg ml^{-1} puromycin and 2 mM 6-DMAP for 4 h, and thereafter, medium containing HDAC inhibitor for 15 h. Culture was performed in a Heracell 150i incubator containing 5% CO2 at 37 °C, in Global medium (IVFonline LGGG-050) containing 10% fetal bovine serum. ES cell derivation was conducted in medium containing DMEM/F12 supplemented with 10% KO-SR and 10% FBS, Rock inhibitor Y-27632, thiazovivin, non-essential amino acids, 10ng ml^{-1} bovine fibroblast growth factor, GlutaMAX, and beta mercaptoethanol (all reagents from Life Technologies). Upon attachment, trophectoderm cells were ablated using laser pulses using a Lykos laser (Hamilton Thorne). Outgrowths were apparent within 10 days of plating, and were picked when colonies reached a size of about 1 mm in diameter. Passaging was done enzymatically using TrpLE (Life Technologies) and standard ES cell medium (substituting FBS with KO-SR and DMEM/F12 with KO-DMEM) using Rock inhibitor Y-27632 for the first day after plating.

IVF embryo culture. The development of IVF embryos was evaluated in a clinical context (Fig. 2a).

Calcium imaging. The removal of the oocyte genome results in a karyoplast containing cytoplasm surrounded by a nuclear envelope. These were placed in a zona pellucida, and incubated in the calcium indicator dye Fluo-4 for 30 min at 37 °C according to the manufacturer's protocol: using the Fluo-4 direct calcium assay kit (Life Technologies), Fluo-4 no wash calcium assay dye solution was mixed 1:1 with Global total. Karyoplasts were imaged both before and after exposure to inactivated Sendai virus using a Nikon TE2000-U microscope with an ET GFP (C92865, 96362) filter and a monochrome camera and exposure time of 200 ms. Contrast was adjusted equally across all images within the same Figure.

Statistical analysis. All oocytes on which experimentation was performed are included in this manuscript. Oocytes were randomly assigned to a specific experimental condition. Oocytes of one donor were used to test 2–3 conditions, depending on the number of oocytes donated. There was no blinding to group allocation. To calculate whether the differences in developmental potential between different experimental conditions were significant, we compared the total number of morulae and blastocysts between different conditions. To reflect the greater developmental progression of a blastocyst versus a morula, each developmental stage was assigned a cell number: 15 for morula stage, 30 for a blastocyst. These numbers were chosen to reflect the greater number of cells contained at each developmental stage (compacted morulae contain approximately 15 cells, blastocysts at least 30 cells). Blastocysts giving rise to stem-cell lines were not given greater weight in this analysis, because blastocysts giving rise to stem-cell lines did not necessarily have a greater cell number (Extended Data Fig. 5). For each condition, the number of morulae was multiplied by factor 15, the number of blastocysts by factor 30. Variables were compared with Chi-square test, and the 95% confidence intervals estimated using Graphpad Prism v. 2.01 (Graphpad Software, USA).

Immunocytochemistry. Oocytes and nuclear transfer cells were analysed using the following antibodies recognizing beta tubulin (Millipore 05-661), anti-centromere (15-235-0001 Antibodies Inc.), phospho-histone H3 Ser 10 (Millipore 06-570), borealin (MBL Int Corp 147-3). Images were taken using a Zeiss LSM710 confocal microscope, or a Zeiss LSM5 Pascal microscope. Immunostaining of human stem-cell lines was done using antibodies for OCT4 (09-0023, Stemgent), nanog (Cell Signaling Technologies D73G4), Tra1-81 (MAB4381 Millipore), and SSEA-4, anti–TRA1-60 (MAB4360; Millipore), PDX1 (R&D AF2419), insulin (Millipore 05-1109), rabbit anti-alpha-fetoprotein (AFP) (A000829; DAKO) and rabbit anti-TUJ1 (T3952; Sigma-Aldrich). Hoechst33342 (Sigma) was used for the staining of DNA, secondary antibodies are from Life Technologies. Cells were fixed in 2%PFA in PBS containing 2.5% Triton-X100 at RT for about 10–15 min. Cells were washed, blocked with FBS and incubated with primary antibodies. Images were taken using an Olympus

IX71 epifluorescence microscope and an Olympus DP30 monochrome camera. Monochrome images were either maintained monochrome (for example, Fig. 2c for the GFP channel), or assigned the colour of the fluorophore (for example, blue for DNA in Fig. 3b). Contrast and intensity were adjusted uniformly across the entire image. Figures were assembled in Adobe Illustrator.

Karyotyping and cell-line analysis. Karyotyping and STR genotyping (Extended Data Table 2) of human cell lines was done by Cell Line Genetics. The karyotype of Fig. 3a required re-labelling of the chromosome numbers because letters provided by Cell Line Genetics are too small for print. Cell lines were tested for mycoplasma contamination using MycoAlert Assay (Lonza) and found to be negative. Gene expression analysis was performed using Illumina HumanHT-12 expression BeadChip and analysed using the Illumina BeadStudio software. Datapoints in Fig. 1 include comparisons to samples from GEO (GSE28024). New data are available at GEO (GSE54849). Gene expression analysis of NT-ES cells and parental fibroblasts was performed using the Human Gene 1.0 ST microarray platform (Affymetrix) according to the manufacturer's protocol. Array data were analysed using Robust Multi-array Average (RMA) in Affymetrix Expression Console and are available at GEO (GSE54876). Comparisons of gene expression levels and principle component analysis included additional published samples, listed in Extended Data Table 1. Neurons were differentiated for 34 days using a modified dual SMAD inhibition protocol[36]. For beta cell differentiation, ES cells were dissociated in trypsin (Gibco), suspended in human ES medium containing 10 μM ROCK inhibitor (Y27632), plated at a density of 150,000 and 800,000 cells per well in 48 and 12-well plates, respectively, and differentiation into definitive endoderm was initiated 24 h later using the STEMdiff definitive endoderm differentiation kit (Stemcell Technologies). Detailed formulations of media used to differentiate definitive endoderm into beta cells were as described previously[37,38]. Insulin secretion upon stimulation with 30 mM KCl was measured by C-peptide ELISA (Mercodia Ultrasensitive C-peptide ELISA, 10-1141-01) according to the manufacturers' instructions, as previously described[38]. Embryoid bodies were generated in DMEM containing 10% FBS and allowed to grow for 3–4 weeks until analysis by immunocytochemistry. For teratoma analysis, stem cells were injected subcutaneously into the dorsal flank of immunocompromised mice NOD.Cg-*Prkdc*^{scid} *Il2rg*^{tm1Wjl}/SzJ (Stock 005557), allowed to grow for 10–15 weeks and then subjected to histological examination with haematoxylin and eosin (HE) staining. No randomization or blinding was used to generate teratomas. Animals were monitored twice weekly for growths and signs of distress. Animal work was approved by the Columbia Institutional Animal Care and Use Committee.

29. Klitzman, R. & Sauer, M. V. Payment of egg donors in stem cell research in the USA. *Reprod. Biomed. Online* **18,** 603–608 (2009).
30. Egli, D. *et al.* Impracticality of egg donor recruitment in the absence of compensation. *Cell Stem Cell* **9,** 293–294 (2011).
31. Choudhary, M. *et al.* Egg sharing for research: a successful outcome for patients and researchers. *Cell Stem Cell* **10,** 239–240 (2012).
32. The Ethics Committee of the American Society for Reproductive Medicine Financial compensation of oocyte donors. *Fertil. Steril.* **88,** 305–309 (2007).
33. Daley, G. Q. *et al.* Ethics. The ISSCR guidelines for human embryonic stem cell research. *Science* **315,** 603–604 (2007).
34. Tachibana, M., Sparman, M. & Mitalipov, S. Chromosome transfer in mature oocytes. *Nature Protocols* **5,** 1138–1147 (2010).
35. Egli, D. & Eggan, K. Nuclear transfer into mouse oocytes. *J. Vis. Exp.* **30,** 116 (2006).
36. Chambers, S. M. *et al.* Highly efficient neural conversion of human ES and iPS cells by dual inhibition of SMAD signaling. *Nature Biotechnol.* **27,** 275–280 (2009).
37. Hua, H. *et al.* iPSC-derived beta cells model diabetes due to glucokinase deficiency. *J. Clin. Invest.* **123,** 3146–3153 (2013).
38. Shang, L. *et al.* Beta cell dysfunction due to increased ER stress in a stem cell model of Wolfram syndrome. *Diabetes* **63,** 923–933 (2014).

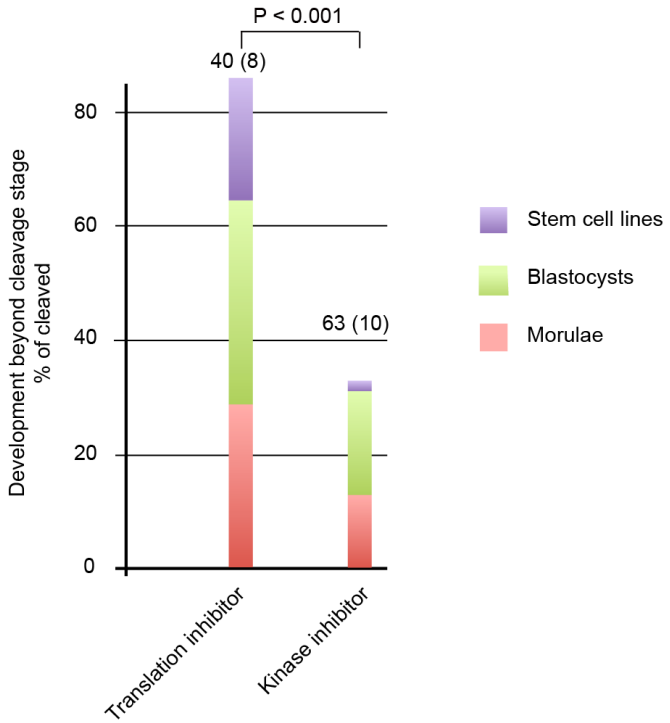

Extended Data Figure 1 | Efficiency of parthenogenetic development beyond the cleavage stage. Shown is the percentage of oocytes giving rise to stem cell lines, blastocysts but no stem cell lines, and morulae as the percentage of the number of oocytes cleaved. Data are from manuscript references[12,14] and displayed here in a direct comparison. The number of oocytes used is indicated above the column. The number of repeats, with oocytes from different donors, is indicated in parenthesis. Statistical analysis using Chi-square test was performed by comparing the total number of cells formed in each condition. Morulae were assigned 15 cells, blastocysts or blastocysts that gave rise to stem-cell lines 30 cells, reflecting the estimated minimal cell count for each group.

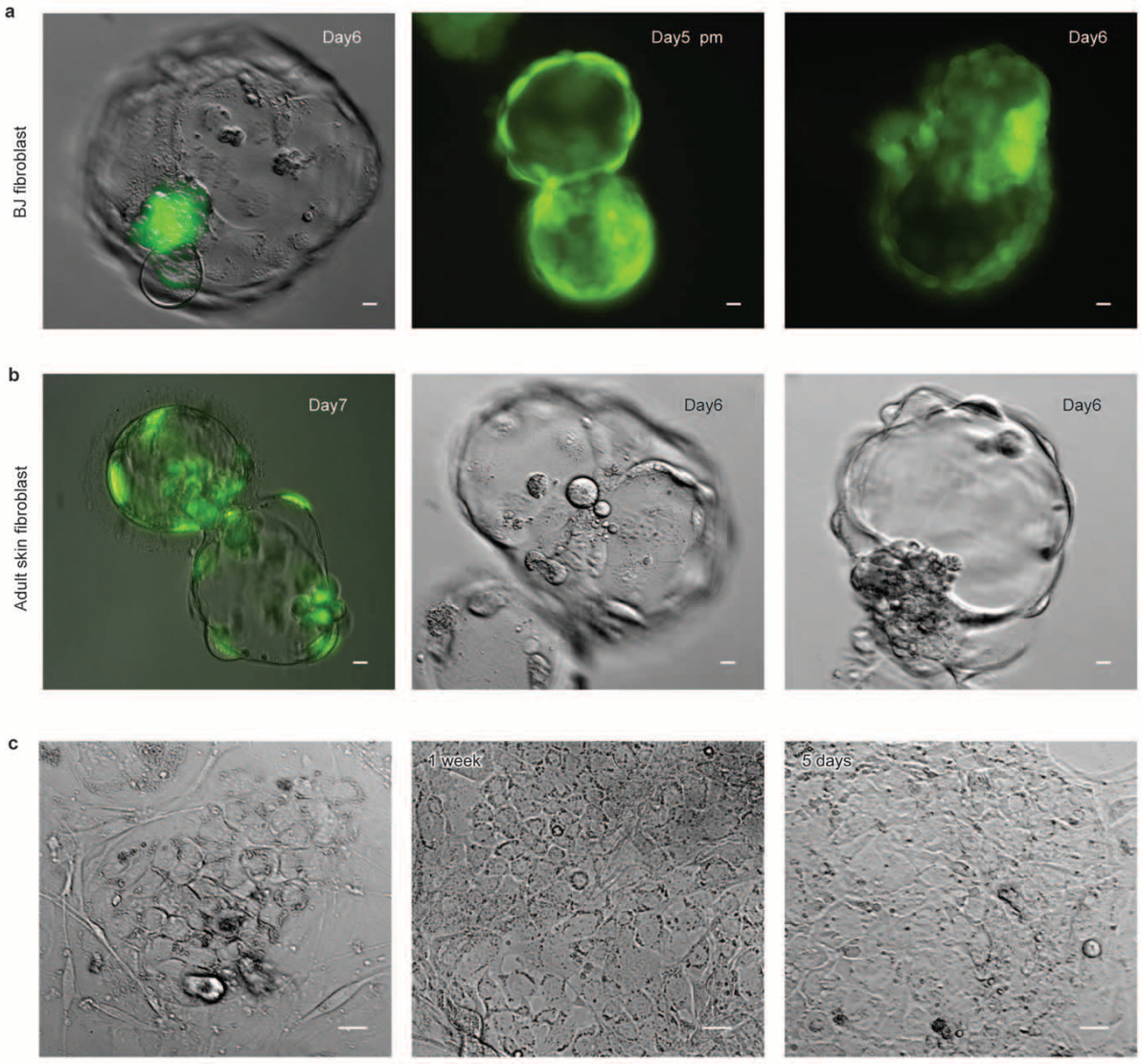

Extended Data Figure 2 | Development to the blastocyst stage and transcriptional activation of the transferred genome. **a**, Blastocyst derived after nuclear transfer of a BJ fibroblast genome (neonatal foreskin fibroblasts). **b**, Blastocysts derived after nuclear transfer of an adult skin fibroblast genome. **c**, Three different nuclear transfer ES cell outgrowths. Time post blastocyst plating is indicated. Scale bar, 10 μm.

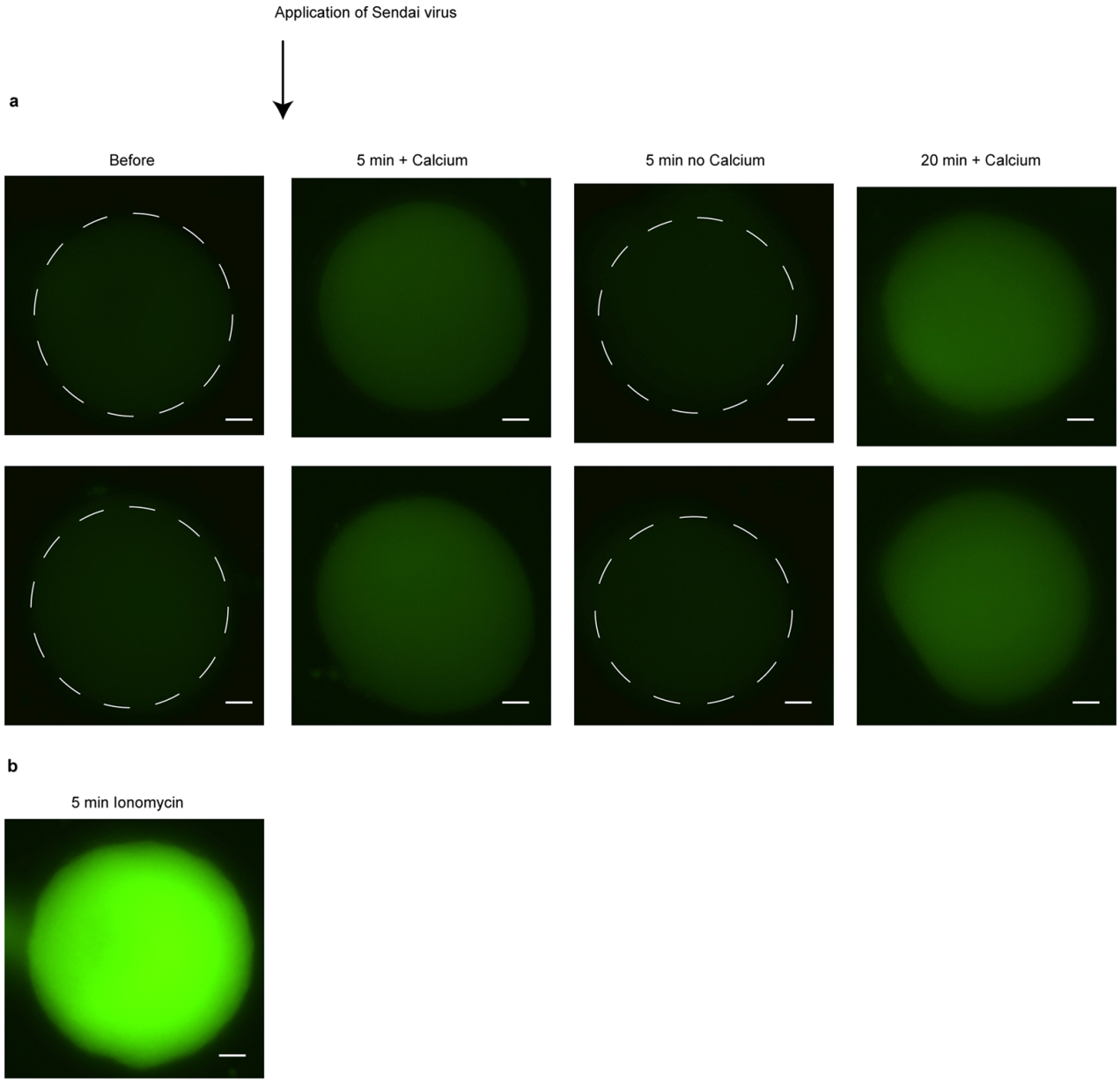

Extended Data Figure 3 | Fluorescence imaging with the calcium-responsive dye Fluo-4. **a**, Human oocytes were incubated in medium containing Fluo-4 for 30 min, imaged for fluorescence, and concentrated Sendai virus was added below the plasma membrane. Shown are two oocytes for each condition or time point. Note that in the absence of calcium in the medium, fluorescence did not increase, whereas a small increase in fluorescence seems to occur in calcium-containing medium. Time point after addition of the virus is indicated. **b**, Incubation of a human oocyte in 3 μM of the calcium ionophore ionomycin as a positive control. Scale bar, 10 μm.

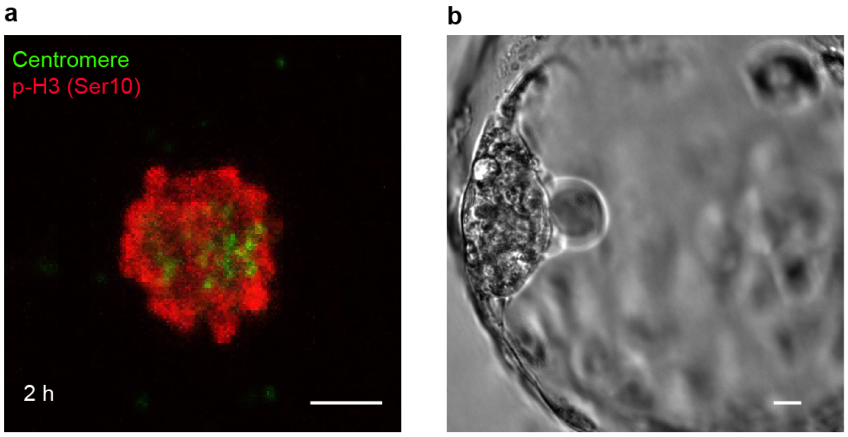

Extended Data Figure 4 | Somatic cell nuclear transfer in the absence of calcium. **a**, Immunochemistry to determine chromosome condensation and histone phosphorylation after transfer of a somatic cell at interphase. Scale bar, 5 μm. **b**, High-quality blastocysts obtained after nuclear transfer with the manipulations conducted in the absence of calcium. Scale bar, 10 μm.

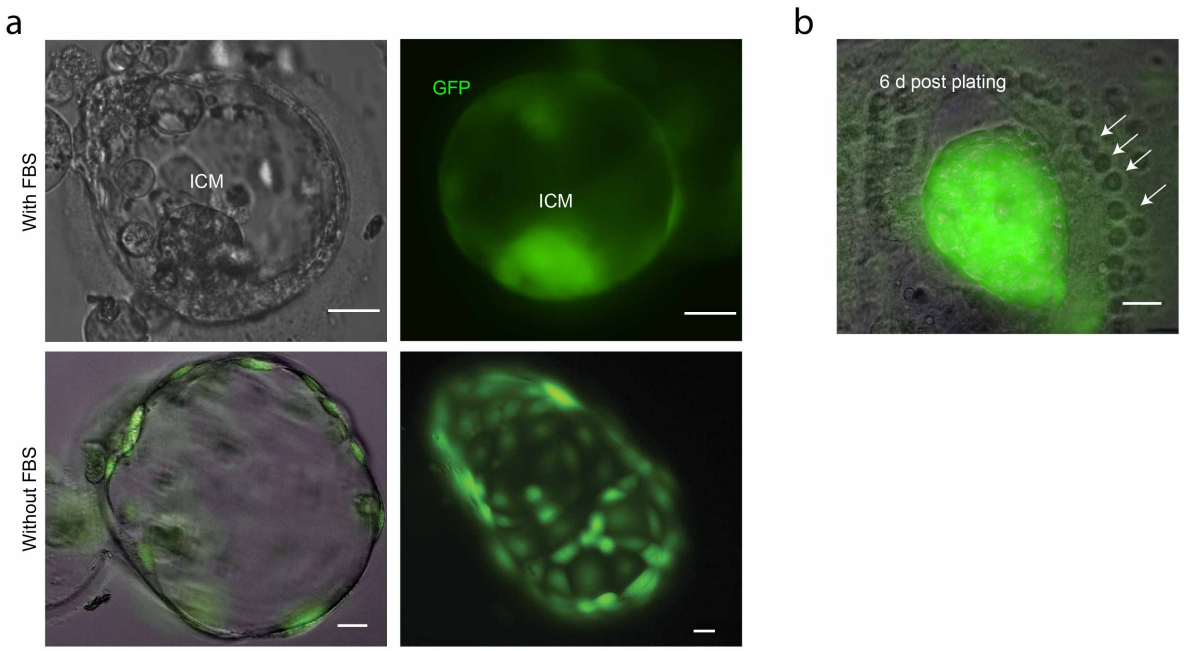

Extended Data Figure 5 | Effect of FBS on blastocyst morphology and ES cell derivation. **a**, Blastocyst generated by somatic cell nuclear transfer in the presence or absence of FBS. **b**, Inner cell mass 6 days post plating. Arrows point to laser marks used to ablate the remaining trophectoderm cells. Scale bar, 20 μm.

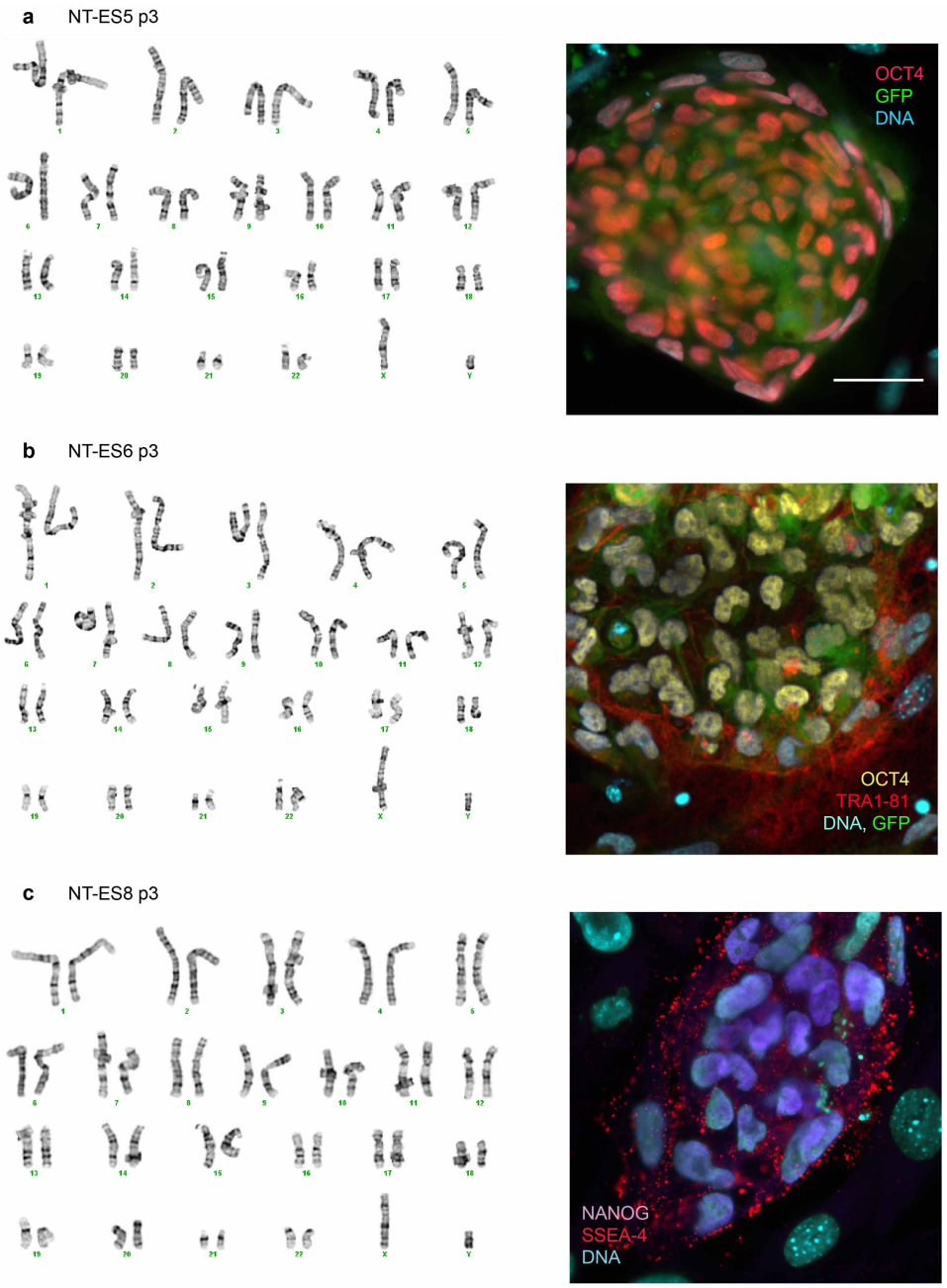

Extended Data Figure 6 | Characterization of NT-ES cells from male foreskin BJ fibroblasts. **a**–**c**, Karyotypes and pluripotency marker expression in three NT-ES cell lines derived from male foreskin BJ fibroblasts. The somatic donor cell used for transfer carries a GFP transgene. Scale bar, 50 μm.

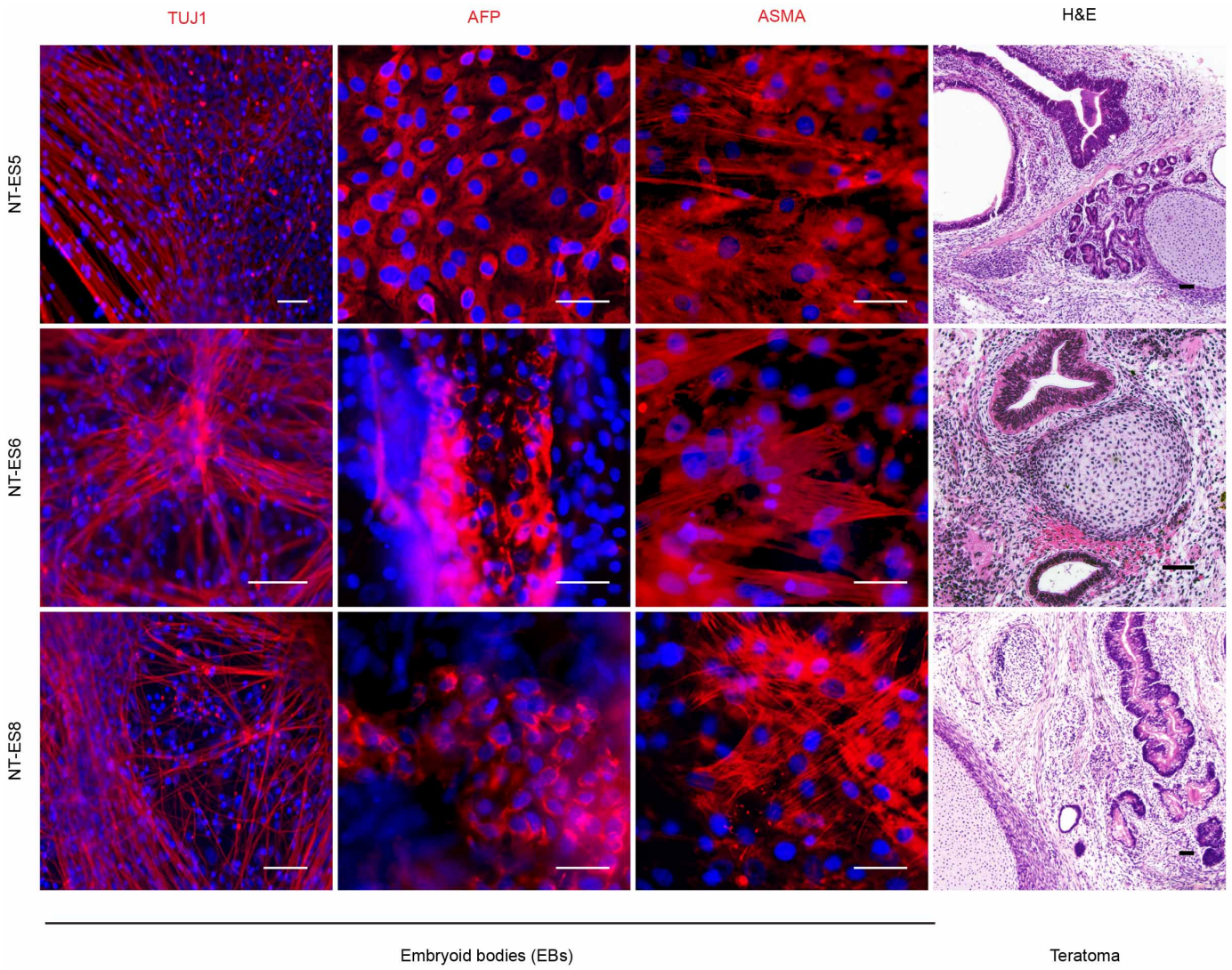

Extended Data Figure 7 | Differentiation of NT-ES cell lines made from male foreskin BJ fibroblasts. Embryoid bodies and teratomas are shown. Scale bar, 50 μm.

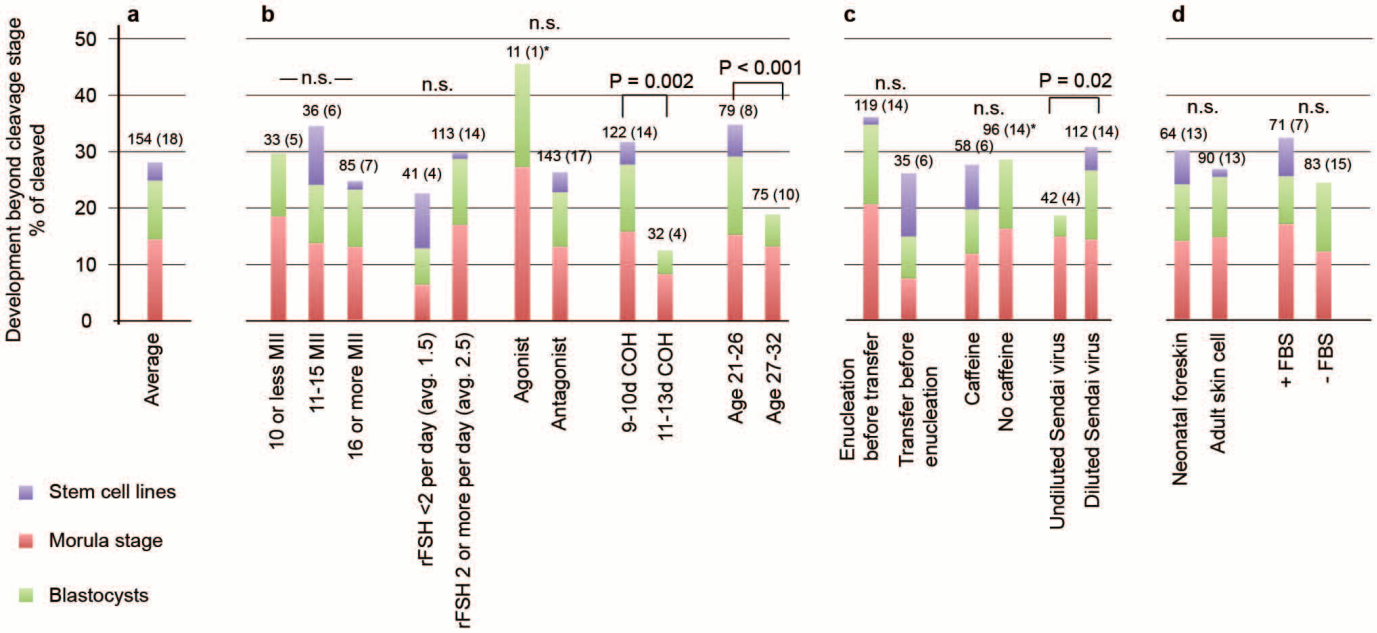

Extended Data Figure 8 | Retrospective analysis of the developmental potential of nuclear transfer oocytes. Shown is the percentage of oocytes developing beyond the cleavage stage, as percentage of eggs progressing beyond the 1-cell stage. Because oocytes of a donor were used to compare two different conditions, if for a particular comparison the added number of oocyte donors exceeds 18, it indicates that these conditions were tested in parallel using oocytes of the same donor. The total number of oocytes used for analysis remained constant. **a**, Average of the 154 oocytes of 18 donors. The total number of 154 oocytes is not equal to the number of oocytes donated by the 18 donors, but is the number of oocytes used for the study of developmental potential after somatic cell nuclear transfer. **b**, Analysis with regard to factors relevant to the hormonal treatment of oocyte donor. **c**, Factors relevant to the manipulation. *Blastocysts generated without caffeine treatment also contained no FBS in the culture medium. Because of the effect of FBS on inner cell mass morphology (Extended Data Fig. 5), FBS is likely the more relevant factor. **d**, Analysis regarding cell source and use of FBS for culture. n.s., non significant. Statistical analysis using Chi-square test was performed by comparing the total number of cells formed in each condition. Morulae were assigned 15 cells, blastocysts or blastocysts that gave rise to stem-cell lines 30 cells, reflecting the estimated minimal cell count for each group.

Extended Data Table 1 | Complete list of samples used in global gene expression analyses

Cell line	GEO accession number	Sample accession number(s)	Publication	Description
BJ-NT-ES-5	GSE54876	GSM1325470 GSM1325471 GSM1325472 GSM1325474	This study	NT-ES cell lines derived from fibroblasts
BJ-NT-ES-6				
BJ-NT-ES-8				
1018-NT-ES				
BJ-Fib		GSM1325473		Fibroblast cell line (BJ)
BJ-iPS-28	GSE21244	GSM531022, GSM531023	Mayshar *et al.Cell Stem Cell 2010*	iPS cell line derived from fibroblasts
H9-ES		GSM531019, GSM531020, GSM531021		ES cell line
BJ-Fib (hTERT)	GSE21348	GSM533418	Urbach *et al.Cell Stem Cell 2010*	Immortalized fibroblast cell line (BJ)
WT-Fib	GSE21037	GSM525415, GSM525416, GSM525417	Marchetto *et al. Cell 2010*	Fibroblast cell line (3 replicates)
iPS-C1		GSM525418, GSM525419, GSM525420		iPS cell lines derived from fibroblasts (3 replicates each)
iPS-C2		GSM525421, GSM525422, GSM525423		
HUES6-ES		GSM525424, GSM525425, GSM525426		ES cell line (3 replicates)
H1-ES	GSE36648	GSM898027, GSM898028, GSM898029	Andrade *et al.Hum Mol Genet. 2010*	ES cell line (3 replicates)
AN1-Fib	GSE48761	GSM1184254, GSM1184255	Cheung *et al.(to be published)*	Fibroblast cell line (AN1) (2 replicates)
AN2-Fib		GSM1184256, GSM1184257		Fibroblast cell line (AN2) (2 replicates)
AN3-Fib		GSM1184258, GSM1184259		Fibroblast cell line (AN3) (2 replicates)
BC-Fib		GSM1184260, GSM1184261		Fibroblast cell line (BC) (2 replicates)
GM03440-Fib		GSM1184262, GSM1184263		Fibroblast cell line (GM03440) (2 replicates)
AN1-iPS		GSM1184274, GSM1184275		iPS cell lines derived from fibroblasts (2 replicates each)
AN2-iPS		GSM1184276, GSM1184277		
AN3-iPS		GSM1184278, GSM1184279		
BC-iPS		GSM1184280, GSM1184281		
GM03440-iPS		GSM1184282, GSM1184283		
CT2-ES		GSM1184302, GSM1184303		ES cell lines (2 replicates each)
ESI-053-ES		GSM1184304, GSM1184305		
H9-ES	GSE20581	GSM517067	Cai *et al.J Biol Chem. 2010*	ES cell line

Extended Data Table 2 | Short tandem repeat (STR) profiles of nuclear transfer ES cell lines

Locus	NT-ES #5	NT-ES #6	NT-ES #8	NT-ES 1018
Amelogenin	XY	XY	XY	X
vWA	16,18	16,18	16,18	16,17
D8S1179	9,11	9,11	9,11	10,15
TPOX	10,11	10,11	10,11	8
FGA	22,23	22,23	22,23	25,27
D3S1358	14,16	14,16	14,16	15,18
THO1	7,8	7,8	7,8	9.3
D21S11	29	29	29	28,30
D18S51	17,19	17,19	17,19	13,15
PentaE	7,17	7,17	7,17	12,14
D5S818	12	12	12	11,13
D13S317	8,9	8,9	8,9	9,11
D7S820	11,12	11,12	11,12	9,10
D16S539	9,13	9,13	9,13	11,13
CSF1PO	10,12	10,12	10,12	10,12
PentaD	12,13	12,13	12,13	9,13